

Cite this: *Chem. Sci.*, 2019, **10**, 1500

All publication charges for this article have been paid for by the Royal Society of Chemistry

Received 10th October 2018  
Accepted 19th November 2018

DOI: 10.1039/c8sc04528c  
[rsc.li/chemical-science](http://rsc.li/chemical-science)

## Characterizing gibberellin flow *in planta* using photocaged gibberellins†

Shira Wexler,<sup>a</sup> Hilla Schayek,<sup>a</sup> Kandhikonda Rajendar,<sup>a</sup> Iris Tal,<sup>a</sup> Eilon Shani,<sup>a</sup> Yasmine Meroz,<sup>a</sup> Roman Dobrovetsky<sup>a</sup> and Roy Weinstain<sup>a</sup>

Gibberellins (GAs) are ubiquitous plant hormones that coordinate central developmental and adaptive growth processes in plants. Accurate movement of GAs throughout the plant from their sources to their destination sites is emerging to be a highly regulated and directed process. We report on the development of novel photocaged gibberellins that, in combination with a genetically encoded GA-response marker, provide a unique platform to study GA movement at high-resolution, in real time and in living, intact plants. By applying this platform to the *Arabidopsis thaliana* endogenous bioactive gibberellin GA<sub>4</sub>, we measure kinetic parameters of its flow, such as decay length and velocity, *in vivo*.

## Introduction

Gibberellins (GAs) are a class of tetra-cyclic di-terpenoid plant hormones that play a major role in regulation of key developmental and adaptive growth processes, including seed germination, organ elongation, transition from vegetative to reproductive growth, and flower, seed, and fruit development.<sup>1–3</sup> Over the years, more than 130 GAs have been identified, of which less than a handful (namely GA<sub>1,3,4,7</sub>) are bioactive.<sup>4</sup> Plants exert multiple layers of regulation (*i.e.* biosynthesis metabolism and perception<sup>4–7</sup>) to coordinate their GA responses in order to achieve appropriate development and growth. Recent evidences, including the identification of specific GA distribution patterns<sup>8,9</sup> and characterization of putative GA transporters,<sup>10–12</sup> suggest that plants also actively and directly regulate the movement of GAs *via* a set of protein transporters to ensure their localized activity. Consequently, understanding the dynamics of GA flow in plants is imperative for an understanding of their regulation and function.

While the long-distance flow of GAs through the phloem sap is extensively being studied,<sup>13–15</sup> the nature of their short-distance movement remains poorly characterized. This is mainly due to a lack of methods with sufficient resolution to introduce and then monitor the movement of GAs, especially *in vivo*. To date, the main approach to quantitatively characterize GA (as well as other plant hormones) short-distance movement has been the application of a radiolabeled GA to a whole plant, or its cut segments, and subsequently quantifying radioactivity

at certain locations and times.<sup>16–20</sup> Such experiments have enabled measuring, for example, the GA<sub>1</sub> flux in oat coleoptiles.<sup>16</sup> While highly sensitive and quantitative, the approach is limited by working with cut plant segments, low resolution and the need to apply the labeled hormone un-naturally from outside the plant, leading to issues of penetration efficiency and time, which complicate the analysis.

Photoactivation (photocaging<sup>21</sup>) has the potential to overcome the limitations associated with traditional applications of bioactive molecules: although caged molecules are introduced from the outside, bioactive molecules are practically released inside the organism, better mimicking endogenous conditions and overcoming penetration issues. In addition, light facilitates unprecedented spatio-temporal control over activation of a caged molecule, enabling initiation of a biological process in a highly defined area and monitoring of it from the get go. Importantly, the technique can be applied to whole, living organisms. We hypothesized that development of photoactivatable GAs will provide an effective way to introduce bioactive GAs directly *in planta* with high spatio-temporal control and, coupled with a fluorescent GA response marker, will facilitate visualization and quantitation of their movement *in vivo* (Fig. 1).

The synthesis of caged gibberellins has been reported twice in the literature.<sup>22,23</sup> The first report describes the synthesis of several GA<sub>3</sub> conjugates, among them to a caging group, yet it focuses on the synthetic feasibility of such molecules' preparation and does not include any evaluation of their functionalities.<sup>22</sup> In the second report, GA<sub>3</sub> was caged with two-photon excitable caging groups,<sup>23</sup> to complement a GA-based chemically induced dimerization (CID) system that was "hijacked" from plants to induce protein degradation in mammalian cells.<sup>24</sup> Understandably, its suitability to the very different physiological conditions in plants has not been evaluated, let alone, its applicability or utility *in planta*.

<sup>a</sup>School of Plant Sciences and Food Security, Faculty of Life Sciences, Tel Aviv University, Tel Aviv 69978, Israel. E-mail: [royweinstain@post.tau.ac.il](mailto:royweinstain@post.tau.ac.il)

<sup>b</sup>School of Chemistry, Raymond and Beverly Sackler Faculty of Exact Sciences, Tel Aviv University, Tel Aviv 69978, Israel

† Electronic supplementary information (ESI) available: Experimental procedures, characterization data, movies and additional figures. See DOI: [10.1039/c8sc04528c](https://doi.org/10.1039/c8sc04528c)



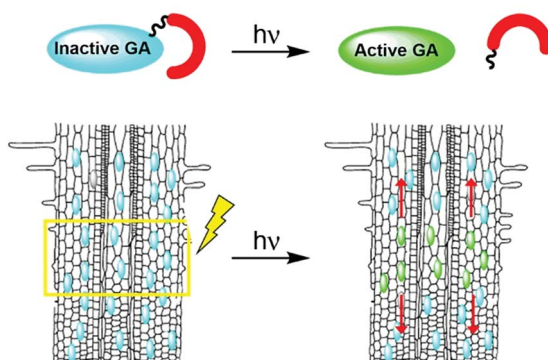


Fig. 1 Schematic representation of bioactive GA photouncaging: (top) general scheme of GA photouncaging, (bottom) direct photo-activation *in planta*, for example in roots, and monitoring of movement thereof.

Here, we optimize the chemical structure required to generate caged gibberellins that are stable *in vivo* in the absence of light, using GA<sub>3</sub> as a model bioactive gibberellin. Based on the resultant insights, we synthesized a caged version of the *Arabidopsis thaliana* endogenous bioactive gibberellin GA<sub>4</sub>, and, in conjunction with a genetically encoded fluorescent GA-response marker, demonstrated real-time monitoring of GA<sub>4</sub> movement in roots of intact, live plants. Furthermore, the technique enabled extraction of quantitative parameters of GA<sub>4</sub> movement over short distances *in planta*.

## Results and discussion

### Design considerations and synthesis of photocaged GA<sub>3</sub>

Design of the caged GA was based on our previous observation that conjugation of a bulky molecule in close proximity to bioactive gibberellins results in the latter's complete loss of function *in vitro* and *in vivo*.<sup>9</sup> We opted for the readily available GA<sub>3</sub> for use as a model bioactive gibberellin and nitrobenzyls as photoprotecting groups<sup>25</sup> because their structural simplicity provides access to diverse derivatives and their small structure adds minimal hydrophobicity to the already hydrophobic GA. We hypothesized that hydrolytic enzymes (*e.g.* esterases) might exist *in planta* that will cleave the ester bond connecting GA<sub>3</sub> to the photo-protecting group, resulting in light-independent activation of GA<sub>3</sub>. We therefore synthesized GA<sub>3</sub> caged with three derivatives of 2-nitrobenzyl, characterized by increasing steric hindrance around the conjugating ester bond (1–3, Fig. 2A), anticipating that more steric hindrance will lead to increased stability *in planta*.

The caged GA<sub>3</sub> derivatives were synthesized by reacting GA<sub>3</sub> with either the appropriate 2-nitrobenzyl bromide (1–2) or 2-nitrobenzyl alcohol (3). Upon 365 nm irradiation, all three compounds effectively released GA<sub>3</sub> with relatively similar overall chemical yields (82%, 85% and 96% for 1–3, respectively, Fig. 2B and C) albeit at different rates ( $t_{1/2} \approx 28, 5.5$  and 5 minutes, respectively). We verified that GA<sub>3</sub> itself does not decompose under such prolonged irradiation conditions (Fig. S1†).

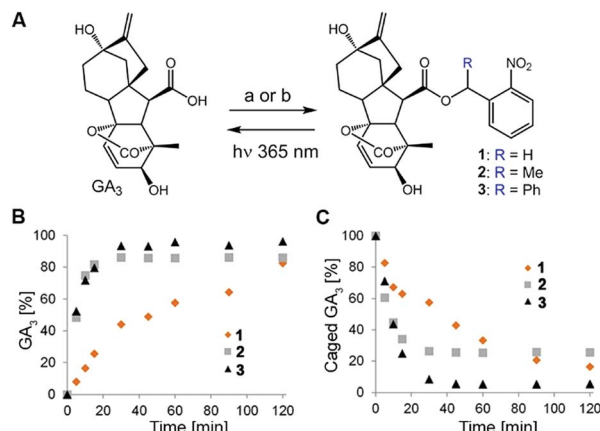
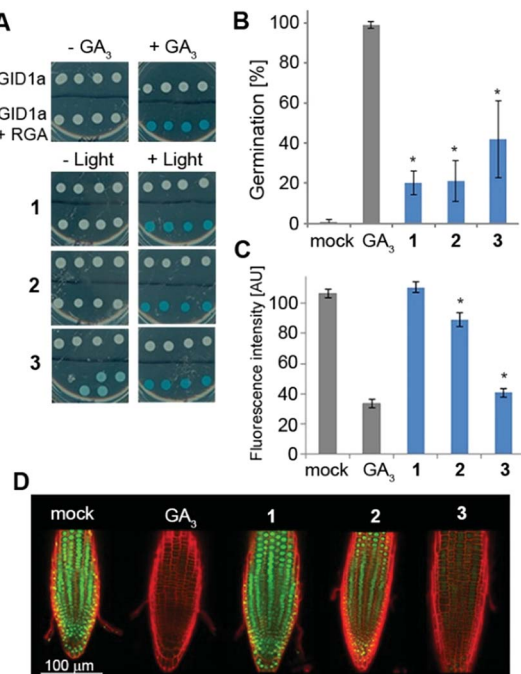


Fig. 2 Caged GA<sub>3</sub> synthesis and uncaging: (A) caged GA<sub>3</sub> was synthesized by reacting GA<sub>3</sub> with either (a) appropriate 2-nitrobenzyl bromide or (b) appropriate 2-nitrobenzyl alcohol. (B and C) Monitoring of caged GA<sub>3</sub> 1–3 photolysis. Formation of GA<sub>3</sub> (B) and disappearance of caged GA<sub>3</sub> (C) upon irradiation with 365 nm light of a 500  $\mu$ M solution of 1–3 in water (10% DMSO, pH 6.4), as monitored by HPLC-MS.

### In vitro and *in vivo* evaluation of caged GA<sub>3</sub> stability

We next studied the derivatives' stability in the absence of light. This is a crucial property as inadvertent release of bioactive molecules completely undermines the utility of the caging strategy. Mechanistically, GA responses in plants are initiated by the binding of a bioactive GA to the receptor GID1 (gibberellin insensitive dwarf 1), promoting its association with repressors of GA responses called DELLA proteins. This association triggers degradation of the DELLA, resulting in activation of the GA responses.<sup>6</sup> In a yeast-two-hybrid (Y2H) system that expresses both GID1a and the DELLA protein RGA (repressor of GAs), we evaluated whether irradiated and non-irradiated caged GA 1–3 would promote the interaction between these two proteins as bioactive GAs do (Fig. 3A). Pre-irradiated 1–3 (25  $\mu$ M) demonstrated robust promotion of the interaction between GID1a and RGA (as evidenced by blue color formation) to the same extent as native GA<sub>3</sub>, confirming that photo-activation leads to release of a functional GA. Importantly, under dark conditions, 1 and 2 did not promote such an interaction, verifying that these caged derivatives are not recognized by the GA's perception mechanism and demonstrating dark stability in this experimental system. Conversely, 3 did promote the GID1a–RGA interaction in the dark, suggesting at least partial hydrolysis of the ester bond and release of free GA<sub>3</sub>. We next evaluated dark stability *in planta*. The GA biosynthesis mutant *ga1-3*, a knockout of the first enzyme in gibberellins' biosynthetic pathway<sup>26</sup> (CPP synthase), germinates poorly due to the absence of an endogenous GA whereas application of an exogenous bioactive GA fully restores its germination competency (Fig. 3B). When *ga1-3* seeds were treated with 1–3 (25  $\mu$ M) for 4 days under light devoid of UV, significantly lower germination levels were observed for 1 and 2 (20% and 21%, respectively) in comparison to 3 (42%), albeit higher than that of the control (0%). Very similar results were





**Fig. 3** Evaluation of caged  $\text{GA}_3$  1–3 stability *in vitro* and *in vivo*. (A) Yeast two-hybrid assay. Yeasts expressing GID1a only or GID1a and RGA were treated: (top) with or without  $25 \mu\text{M}$   $\text{GA}_3$  and (bottom) with  $25 \mu\text{M}$  1–3 pre-irradiated (+light) or not (−light). (B) Germination assay. *Ler ga1-3* mutant seeds ( $n = 30$ –50) were sown on MS plates containing  $25 \mu\text{M}$  1–3. The germination status was determined on day 4. Mock represents no treatment. Error bars represent STDV. (C) GFP-RGA response to 1–3 in dark grown root tips. *pRGA:GFP-RGA* *Arabidopsis* seedlings ( $n = 6$ –8) were treated with paclobutrazol (paclo,  $2 \mu\text{M}$ ) overnight and subsequently transferred to MS plates containing paclo ( $2 \mu\text{M}$ ) and any of the 1–3 ( $25 \mu\text{M}$ ). Images were taken after 4 hours. Mock represents no treatment. Error bars represent SEM. \*Statistical significance (one-way ANOVA with Tukey correction,  $p < 0.05$ ) from  $\text{GA}_3$  (B) or mock (C). (D) Representative images of the data in (C). Red: propidium iodide (PI). Green: GFP-RGA.

observed in a root elongation assay (Fig. S2†), implying that **1** and **2** are more resistant to hydrolysis *in planta* than **3**. In an effort to tease out a stability difference between **1** and **2**, we utilized the genetically encoded GA marker GFP-RGA. The fused green fluorescent protein (GFP) and RGA serves as a “turn-off” marker for GAs; in the absence of GAs, GFP-RGA is stable and can be readily detected while in the presence of GAs, the fusion protein is degraded and the fluorescence signal diminishes.<sup>27</sup> Treatment of transgenic *Arabidopsis* seedlings expressing GFP-RGA under RGA’s native promoter (*pRGA:GFP-RGA*) with **1**–**3** ( $25 \mu\text{M}$ ) revealed a significant difference; while **2** led to an  $\sim$ 20% reduction in the fluorescence signal, **1** was completely stable at this time point and **3** showed the lowest fluorescence signal (Fig. 3C and D).

#### Susceptibility to acidic hydrolysis correlates with caged GA stability *in planta*

The assays described above reveal a clear trend of *in planta* stability with an inverse correlation to steric hindrance around the ester bond (**1** > **2** > **3**), suggesting that enzymatic cleavage is

not the cause for degradation of the conjugates as was initially hypothesized. Since the apoplast (extracellular space) in plants is a low pH environment (*ca.* 5.5 (ref. 28)), we speculated that ester hydrolysis through an acidic mechanism could be responsible for degradation of the conjugates. To explore this assumption, we performed density functional theory (DFT) calculations of the potential energy surface (PES) of the hydrolysis of the model systems **1a**–**3a** at the B3LYP/6-31(d) level of theory in water using a conductor-like polarizable continuum model (CPCM) (Fig. 4A). The results show that formation of the orthoesters is the rate determining step (RDS) of the hydrolysis reaction and is exergonic for all three model compounds ( $\Delta G = 8.29$ ,  $7.98$  and  $5.11 \text{ kcal mol}^{-1}$ , respectively). The calculated barriers of the RDS for the hydrolysis of **1a** is  $1.57 \text{ kcal mol}^{-1}$  higher than that for **2a** and  $3.41 \text{ kcal mol}^{-1}$  higher than that for **3a**. Thus, the barriers of the RDSs for the hydrolysis of esters of the order **1a** > **2a** > **3a** clearly reflect the difference in hydrolysis rates (**1** > **2** > **3**) observed *in planta*. Moreover, incubation of **1**–**3** in liquid MS medium (pH 5.5) further corroborated the differences in the hydrolysis rate: **1** being slightly more resistant than **2** while **3** hydrolyses comparatively quickly (Fig. 4B). Collectively, both DFT calculations and experimental results point towards susceptibility to acidic hydrolysis as the determinant of GA conjugate stability *in planta*. This insight should be highly valuable in designing controlled-release conjugates of GAs.

#### Caged $\text{GA}_4$ can be effectively photolyzed *in planta*

Although  $\text{GA}_3$  is a bioactive gibberellin, it is not endogenous to *Arabidopsis thaliana*. Previous studies have shown that putative GA transporters have differential specificity and activity towards distinct GAs, and therefore, GA variants are expected to be transported differentially *in planta*.<sup>29,30</sup> Thus, in order to study the short-distance movement of a bioactive GA in its proper context, we synthesized a caged version of  $\text{GA}_4$ , the endogenous and most abundant bioactive GA in *Arabidopsis*,<sup>31</sup> in a similar manner to **1** (**4**, Fig. 5A). We first evaluated the stability of **4** in *Arabidopsis* seedlings. Transgenic *pRGA:GFP-RGA* seedlings were treated for 15 minutes with an increasing concentration of **4** ( $5$ – $50 \mu\text{M}$ ) and imaged 90 minutes later. At concentrations above  $10 \mu\text{M}$ , a significant decrease in the GFP signal was observed, suggesting partial hydrolysis of **4** and release of  $\text{GA}_4$  in sufficient amounts to be detected (Fig. S3†). At lower concentrations however ( $2.5$  and  $5 \mu\text{M}$ ), no change in the GFP fluorescence signal was observed for at least 3 hours (Fig. 5B and S4†), indicating the hydrolysis rate below the detection limit of the marker. These results provide a time-window of at least 3 hours for *in vivo* experiments using the optimized concentration of **4**. We next tested photoactivation of **4** *in planta*. Transgenic *pRGA:GFP-RGA* seedlings were treated for 15 minutes with **4** ( $2.5$  and  $5 \mu\text{M}$ ); their root tips were irradiated using a confocal lamp ( $365/10 \text{ nm}$ ,  $2 \text{ mW cm}^{-2}$ ) for increasing periods of time and imaged 90 minutes later. Light exposure for  $>5$  seconds resulted in a decrease in the GFP fluorescence signal to the same level observed in seedlings treated directly with  $\text{GA}_4$  ( $2.5 \mu\text{M}$ ) (Fig. 5C and D and S5†). Importantly, seedlings that were exposed to similar irradiation conditions but in the absence of **4** showed no

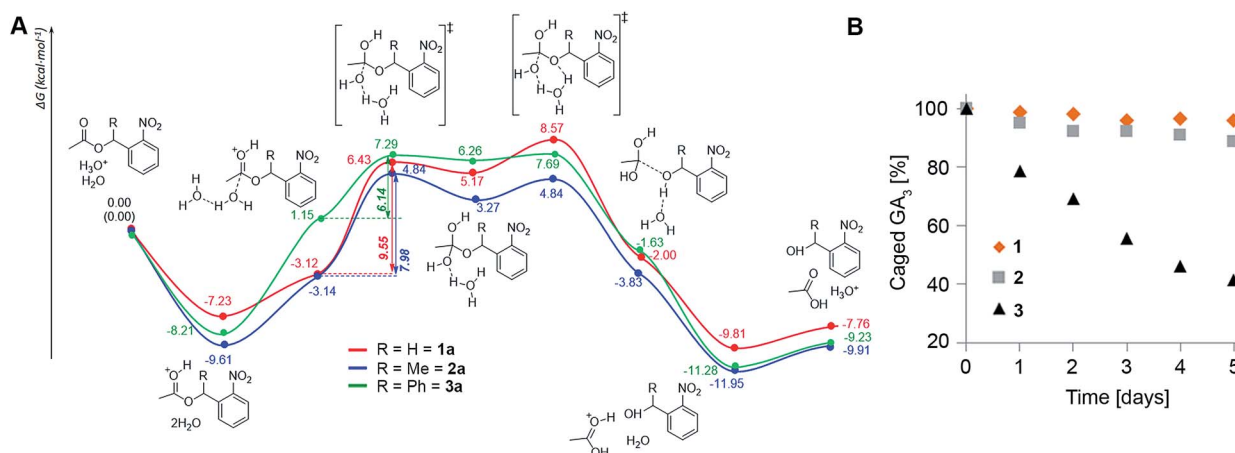


Fig. 4 Susceptibility to acidic hydrolysis determines caged GA stability *in vivo*. (A) DFT calculated PES of hydrolysis reactions of **1a**–**3a**. Gibbs free energies in kcal mol<sup>-1</sup> are given relative to the starting materials. (B) Caged GA<sub>3</sub> stability at low pH. Caged GA<sub>3</sub> **1**–**3** (100  $\mu$ M in liquid 1/2 MS medium, 1% DMSO) as monitored by HPLC-MS at indicated times.

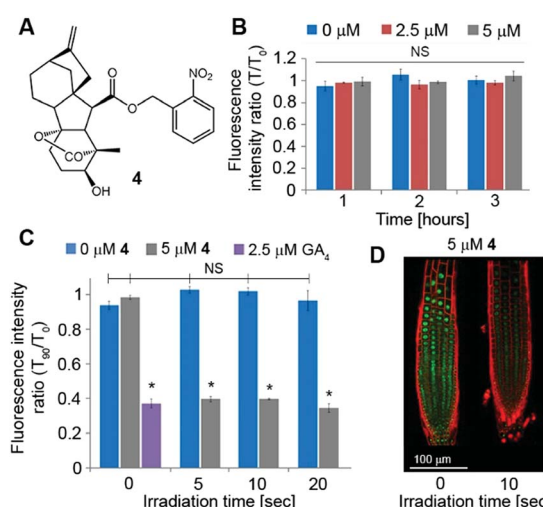


Fig. 5 Photoactivation of caged GA<sub>4</sub> *in vivo*: (A) structure of caged GA<sub>4</sub>. (B–D) Dark stability and photoactivation of **4** *in vivo*. 4 days old *pRGA:GFP-RGA* *Arabidopsis* seedlings ( $n = 3$ ) were treated with paclit (2  $\mu$ M) overnight and incubated with **4** at indicated concentrations for 15 minutes. (B) Seedlings were kept in the dark until imaged at indicated times. (C) Seedling roots were irradiated using a confocal lamp (365/10 nm, 2 mW cm<sup>-2</sup>) for indicated times. Root tips were imaged 90 minutes later. Error bars represent SEM. \*Statistical significance (one-way ANOVA with Tukey correction,  $p < 0.05$ ) from the  $T_0$  of 0  $\mu$ M **4**. (D) Representative images of plants treated with 5  $\mu$ M **4** in (C). Red: PI. Green: GFP-RGA.

decrease in their GFP-RGA signal and revealed no signs of phototoxicity even at the highest light dosage, as determined by a follow-up root elongation assay (Fig. S6†). The response of the GA marker to the photoreleased GA<sub>4</sub> could be monitored in real time (Movies S1, S2†), providing a platform to study its movement at high-resolution. Collectively, these results establish that a tunable pulse of bioactive GA<sub>4</sub> can be successfully generated *in planta* by light control and that its movement from the activation point can be monitored in real time. This is the first demonstration of *in vivo* light-mediated control over this central plant hormone.

### Quantitation of GA<sub>4</sub> movement in *Arabidopsis* roots

We next sought to utilize our technique's optimized parameters to extract kinetic properties of GA<sub>4</sub> movement in roots of intact *Arabidopsis* plants. We first turned to evaluate the GA decay length in the root, a parameter that provides information about the remoteness at which these hormones can act. As weak acids, GAs tend to get trapped inside cells, where the relatively high pH (~7.0) limits them from crossing into the apoplast. This "ion-trap" mechanism<sup>29</sup> restricts the distance to which GAs can diffuse. The fraction of the GA that can cross a distance  $x$  through the apoplast  $f(x)$  was previously defined<sup>32</sup> as

$$f(x) = 10^{-x/L_{\text{apo}}} \quad (1)$$

where  $L_{\text{apo}}$  is a characteristic decay length. By theoretically estimating parameters such as the GA diffusion coefficient and thickness and permeability of plant cell walls, it was calculated that the value of  $L_{\text{apo}}$  is in the order of 20–60  $\mu$ m. This very short theoretically calculated decay length has prompted the assumption that active exporters of a GA should exist in order to enable it to travel further distances.<sup>29,33</sup>

We postulated that our experimental system will allow us to directly measure  $f(x)$  for different distances  $x$  and thus, extract  $L_{\text{apo}}$  based on experimental observations. For this, transgenic *pRGA:GFP-RGA* seedlings were treated with **4** (5  $\mu$ M) and irradiated (365/10 nm, 2 mW cm<sup>-2</sup>, 10 s) at increasing distances from the root tip ( $x = 0.28$ – $0.93 \pm 0.05$  mm, Fig. 6A). The GFP-RGA signal was monitored at the root tip and quantified. The results showed that both the extent and rate of the marker response at the root tip decreases as the distance of the photoactivation location from the root tip increases (Fig. 6B). Since the intensity of the marker response is correlated with the amount of GA present, we substituted  $f(x)$  with the marker response for each distance  $x$  in eqn (1) thus extracting  $L_{\text{apo}} = 1.6 \pm 0.4$  mm (for a detailed calculation, see the ESI†). The finding that the observed  $L_{\text{apo}}$  is 1.5–2 orders of magnitude higher than the theoretically calculated one (which assumes no active transport) provides additional, experimental support to the

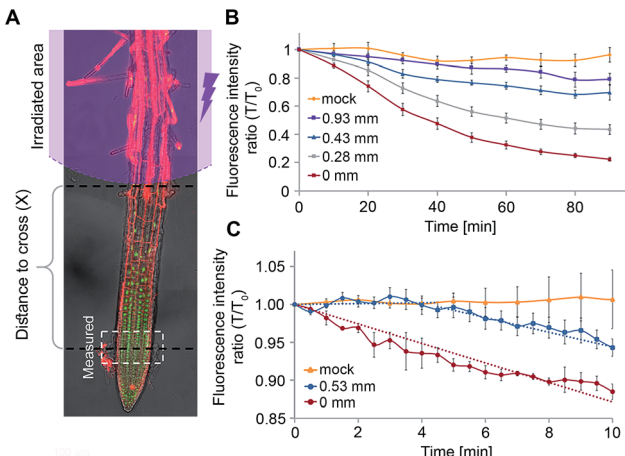


Fig. 6 Quantitation of GA<sub>4</sub> movement properties *in vivo*: (A) schematic illustration of the experimental setup for characterizing GA<sub>4</sub> movement. (B and C) Fluorescence response of GFP-RGA at the root tip following photoactivation of **4** (5  $\mu$ M, 365/10 nm, 2 mW  $\text{cm}^{-2}$ , 10 s) at indicated distances, measuring the decay length (B) or velocity (C). Error bars represent SEM.

assumption that active transport of GAs takes place, enabling GAs to overcome the “ion-trap” mechanism and travel relatively long distances *in planta*.

We utilized a similar experimental setup to measure the GA<sub>4</sub> velocity in the root. This is an important parameter in defining which GA biosynthesis sites contribute to a GA response in a specific location. To be relevant, a GA must be able to cross the distance from its source to destination within the time-frame of a response initiation. Photoactivation of **4** at a known distance from the root tip ( $0.53 \pm 0.05$  mm) and monitoring of the marker at higher frequency (every 30 seconds) revealed a delay of  $4 \pm 1$  minute in the marker's response compared to its photoactivation at the site of monitoring (0 mm, Fig. 6C). The observed lag time mostly represents the time required for GA<sub>4</sub> to cross this distance, thus enabling determining a minimal velocity of  $8.0 \pm 2.0$  mm  $\text{h}^{-1}$  for GA<sub>4</sub> in the root tip. To the best of our knowledge, this is the first measurement of GA<sub>4</sub> velocity in whole, live plants. The observed velocity is comparable to that measured for auxin in *Arabidopsis* roots ( $9 \pm 1$  mm  $\text{h}^{-1}$  (ref. 20 and 34)) and higher than that previously reported for GA<sub>3</sub> in cut Coleus petioles ( $1.4$  mm  $\text{h}^{-1}$  (ref. 35)).

## Conclusions

In summary, we have established a conceptually novel platform to study the movement of bioactive GAs in whole, living plants. Development of photocaged gibberellins and their combination with a genetically encoded GA-response marker, enabled monitoring of the hormone's movement at high-resolution and in real time in living, intact plants. This technique was applied to quantitate kinetic properties of an endogenous gibberellin flow in roots, such as its decay length and velocity. These data will facilitate a better understanding of GA regulation and function in plants as well as provide concrete, experimental

information to support development of computational models for GA flow. We expect that improving the spatial-resolution of caged GA photoactivation by switching to visible light-exitable photocages, along with replacement of the GA marker with a faster and more sensitive one,<sup>33</sup> would significantly enhance the technique's accuracy and its capacity to unveil higher-resolution details of GA flow. We further anticipate that a similar approach could be taken to study other hormones and bioactive small-molecules in plants.

## Conflicts of interest

There are no conflicts to declare.

## Acknowledgements

We would like to thank the German-Israel Foundation (I-2387-302.5/2015), the European Research Council (679189) and the Israeli Science Foundation (1832/14) for funding this research.

## Notes and references

- P. Achard and P. Genschik, *J. Exp. Bot.*, 2009, **60**, 1085–1092.
- J. M. Daviere and P. Achard, *Development*, 2013, **140**, 1147–1151.
- P. Hedden and V. Sponsel, *J. Plant Growth Regul.*, 2015, **34**, 740–760.
- S. Yamaguchi, *Annu. Rev. Plant Biol.*, 2008, **59**, 225–251.
- K. Murase, Y. Hirano, T. P. Sun and T. Hakoshima, *Nature*, 2008, **456**, 459–463.
- T. P. Sun, *Plant Physiol.*, 2010, **154**, 567–570.
- M. Ueguchi-Tanaka, M. Ashikari, M. Nakajima, H. Itoh, E. Katoh, M. Kobayashi, T. Y. Chow, Y. I. Hsing, H. Kitano, I. Yamaguchi and M. Matsuoka, *Nature*, 2005, **437**, 693–698.
- L. Matias-Hernandez, A. E. Aguilar-Jaramillo, M. Osnato, R. Weinstain, E. Shani, P. Suarez-Lopez and S. Pelaz, *Plant Physiol.*, 2016, **170**, 1624–1639.
- E. Shani, R. Weinstain, Y. Zhang, C. Castillejo, E. Kaiserli, J. Chory, R. Y. Tsien and M. Estelle, *Proc. Natl. Acad. Sci. U. S. A.*, 2013, **110**, 4834–4839.
- Y. Chiba, T. Shimizu, S. Miyakawa, Y. Kanno, T. Koshiba, Y. Kamiya and M. Seo, *J. Plant Res.*, 2015, **128**, 679–686.
- Y. Kanno, T. Oikawa, Y. Chiba, Y. Ishimaru, T. Shimizu, N. Sano, T. Koshiba, Y. Kamiya, M. Ueda and M. Seo, *Nat. Commun.*, 2016, **7**, 13245.
- I. Tal, Y. Zhang, M. E. Jorgensen, O. Pisanty, I. C. Barbosa, M. Zourelidou, T. Regnault, C. Crocoll, C. E. Olsen, R. Weinstain, C. Schwechheimer, B. A. Halkier, H. H. Nour-Eldin, M. Estelle and E. Shani, *Nat. Commun.*, 2016, **7**, 11486.
- J. Dayan, N. Voronin, F. Gong, T. P. Sun, P. Hedden, H. Fromm and R. Aloni, *Plant Cell*, 2012, **24**, 66–79.
- L. Ragni, K. Nieminen, D. Pacheco-Villalobos, R. Sibout, C. Schwechheimer and C. S. Hardtke, *Plant Cell*, 2011, **23**, 1322–1336.

15 T. Regnault, J. M. Daviere, M. Wild, L. Sakvarelidze-Achard, D. Heintz, E. Carrera Bergua, I. Lopez Diaz, F. Gong, P. Hedden and P. Achard, *Nat. Plants*, 2015, **1**, 15073.

16 G. A. Drake, *J. Exp. Bot.*, 1979, **30**, 429–437.

17 G. A. Drake and D. J. Carr, *J. Exp. Bot.*, 1979, **30**, 439–447.

18 W. P. Jacobs and P. E. Pruett, *Am. J. Bot.*, 1973, **60**, 896–900.

19 M. Kwiatkowska, *Planta*, 1991, **183**, 294–299.

20 E. M. Kramer, H. L. Rutschow and S. S. Mabie, *Trends Plant Sci.*, 2011, **16**, 461–463.

21 J. H. Kaplan, B. Forbush IIIrd and J. F. Hoffman, *Biochemistry*, 1978, **17**, 1929–1935.

22 J. L. Ward and M. H. Beale, *Phytochemistry*, 1995, **38**, 811–816.

23 K. M. Schelkle, T. Griesbaum, D. Ollech, S. Becht, T. Buckup, M. Hamburger and R. Wombacher, *Angew. Chem., Int. Ed.*, 2015, **54**, 2825–2829.

24 T. Miyamoto, R. DeRose, A. Suarez, T. Ueno, M. Chen, T. P. Sun, M. J. Wolfgang, C. Mukherjee, D. J. Meyers and T. Inoue, *Nat. Chem. Biol.*, 2012, **8**, 465–470.

25 P. Klan, T. Solomek, C. G. Bochet, A. Blanc, R. Givens, M. Rubina, V. Popik, A. Kostikov and J. Wirz, *Chem. Rev.*, 2013, **113**, 119–191.

26 T. Sun, H. M. Goodman and F. M. Ausubel, *Plant Cell*, 1992, **4**, 119–128.

27 A. L. Silverstone, H. S. Jung, A. Dill, H. Kawaide, Y. Kamiya and T. P. Sun, *Plant Cell*, 2001, **13**, 1555–1566.

28 Q. Yu, C. Tang and J. Kuo, *Plant Soil*, 2000, **219**, 29–40.

29 J. Binenbaum, R. Weinstain and E. Shani, *Trends Plant Sci.*, 2018, **23**, 410–421.

30 A. Rizza and A. M. Jones, *Curr. Opin. Plant Biol.*, 2018, **47**, 9–15.

31 M. Talon, M. Koornneef and J. A. Zeevaart, *Proc. Natl. Acad. Sci. U. S. A.*, 1990, **87**, 7983–7987.

32 E. M. Kramer, *Plant Physiol.*, 2006, **141**, 1233–1236.

33 A. Rizza, A. Walia, V. Lanquar, W. B. Frommer and A. M. Jones, *Nat. Plants*, 2017, **3**, 803–813.

34 A. M. Rashotte, J. Poupart, C. S. Waddell and G. K. Muday, *Plant Physiol.*, 2003, **133**, 761–772.

35 W. P. Jacobs, *The Movement of Plant Hormones: Auxins, Gibberellins, and Cytokinins*, Berlin, Heidelberg, 1972.

